Mara Bruzzi

CSN5 Experiments on Detectors & Dosimeters in 2021

(3DSIAM, PERO2, SAMADHA and TIMESPOT)

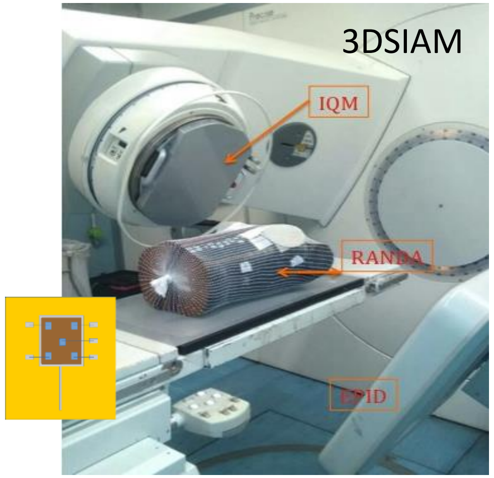

Primary focuses of CSN5

- **Development of radiation detectors, accelerators, electronics and computer technology;**
- **applications in physics and interdisciplinary research as medical physics, environment and cultural heritage protection**

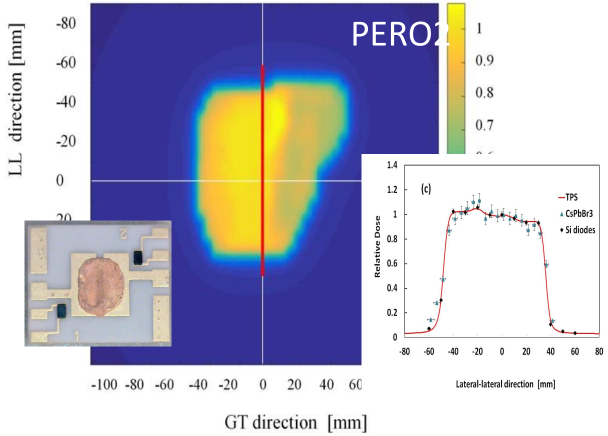

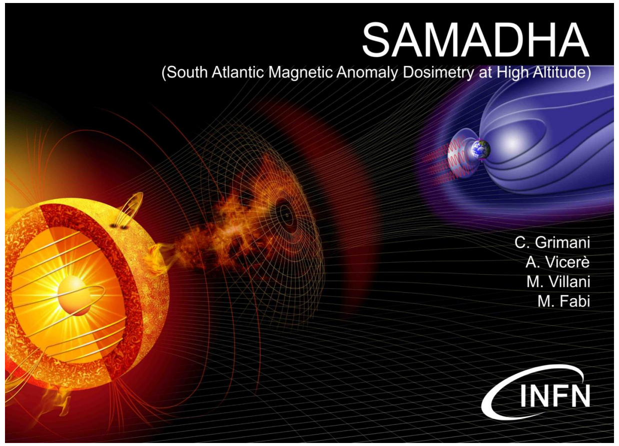

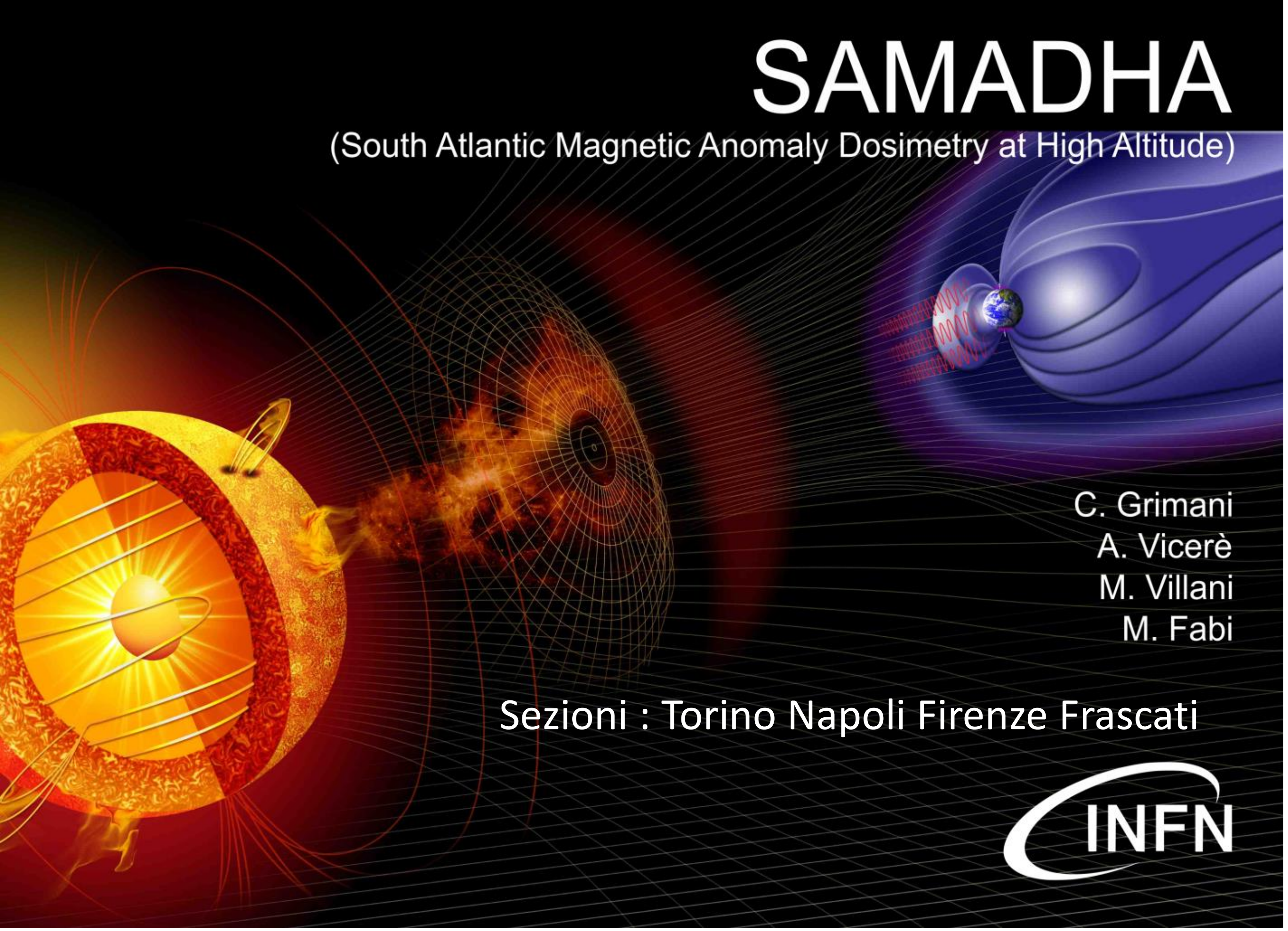

- **Scientific objectives:** the aim of the SAMADHA experiment is to measure the dose absorbed by South America population due to secondary cosmic rays and proton precipitation from the inner Van Allen belt in the region of the *South Atlantic Anomaly* (SAA).
- **Background:** this experiment follows HALCORD funded by INFN (*High Altitude and Latitude Cosmic Ray Dosimetry*, 2017-2019)

Role of the Florence group: Preparation of an analysis tool for space data (Solar Orbiter SWA+EPD+METIS) and ground data (SAMADHA and south pole neutron monitors) correlation and interpretation in terms of interplanetary processes (mainly the first year, an analogous study is needed for LISA) and simulation with Fluka of active dosimeters Liulin (first and second year)

Project Responsible for INFN Firenze C. Grimani

SAMADHA measurement sites

Performing dosimetric measurements, with a particular attention to the neutron dose, at very high mountain altitude in the region of the South Atlantic Anomaly (SAA).

Chacaltaya
5240 m a.s.l.
Bolivia, 16.35° S, 68.13° W

Monte Famatina
5100 m a.s.l.
Argentina, 28.92° S, 67.52° W

Geomagnetic field and South Atlantic Anomaly

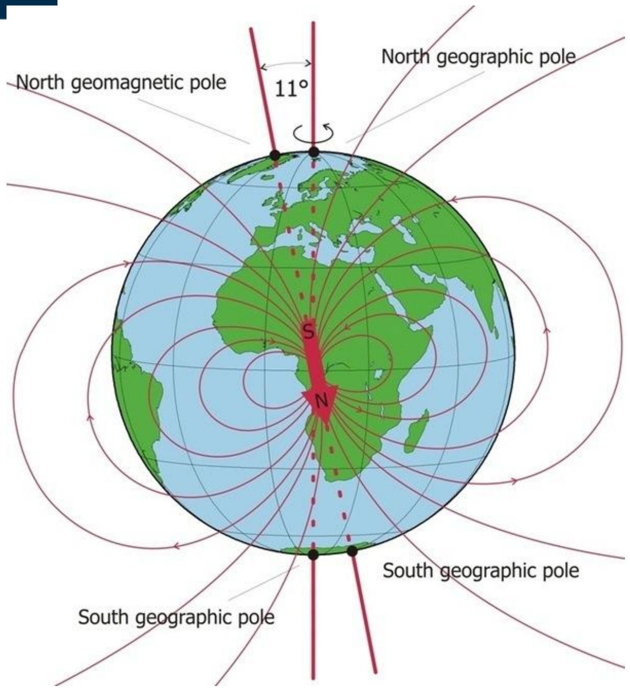

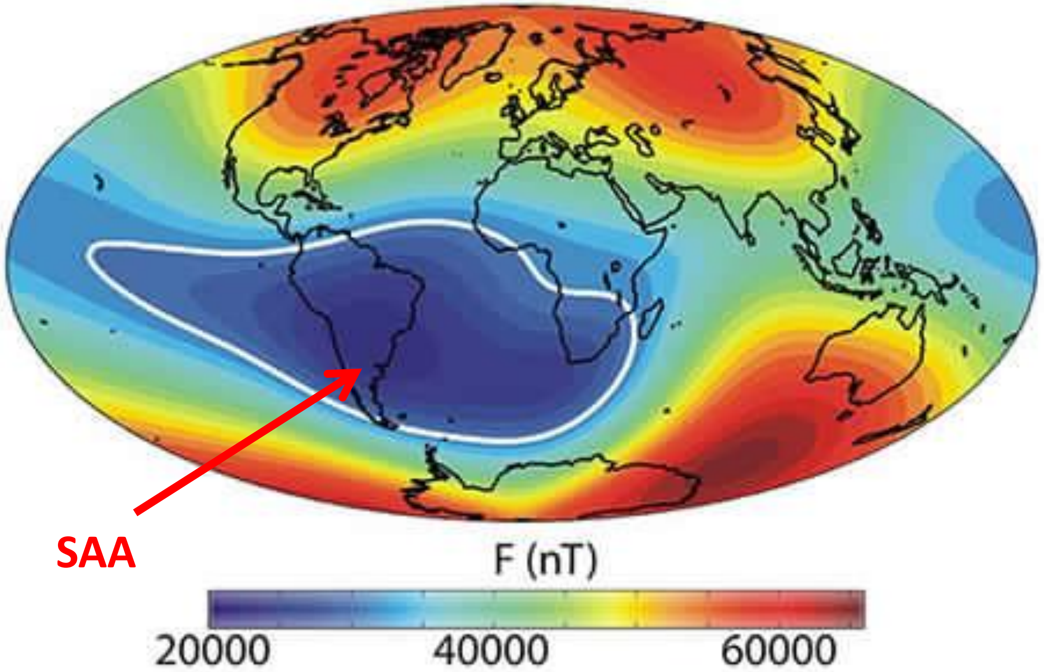

At the Earth's surface the main field can be approximated by a dipole placed close to the Earth's center and tilted to the axis of rotation by about 11°.

The dipole center is displaced by ≈500 km with respect to the Earth center and for this asimmetry, there is a region where the field has a minimum: the South Atlantic Anomaly.

Project Responsible for INFN Firenze C. Grimani

SAA evolution in the last two centuries

In the last century the geomagnetic dipole is weakening.

In particular, the intensity of the minimum magnetic field in the SAA is decreasing, and the area of the SAA is increasing.

The point with the minimum magnetic field intensity is drifting westward.

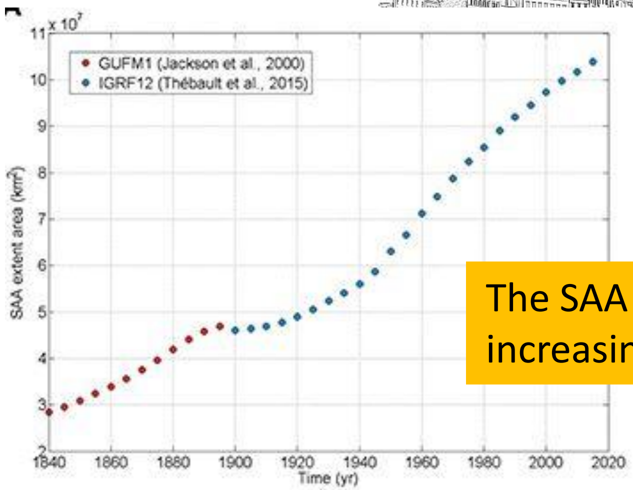

The SAA area is increasing

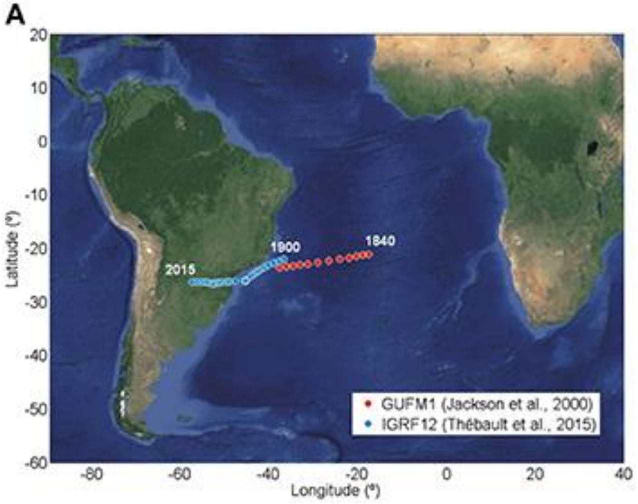

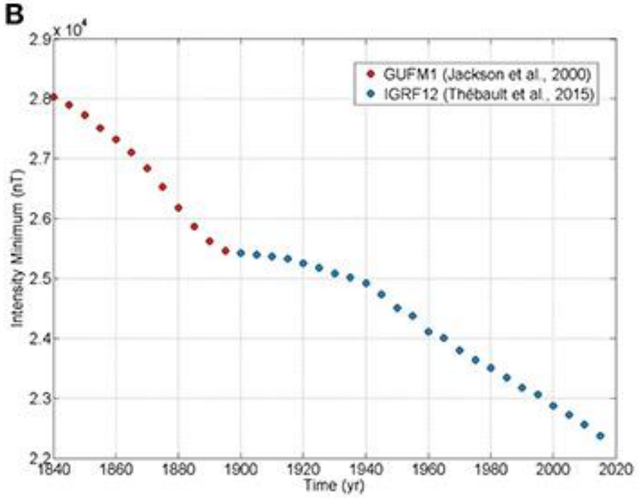

The value of the minimum magnetic field in the SAA is decreasing

F. Javier Pavón-Carrasco and Angelo De Santis,2016

Project Responsible for INFN Firenze C. Grimani

Van Allen belts and South Atlantic Anomaly

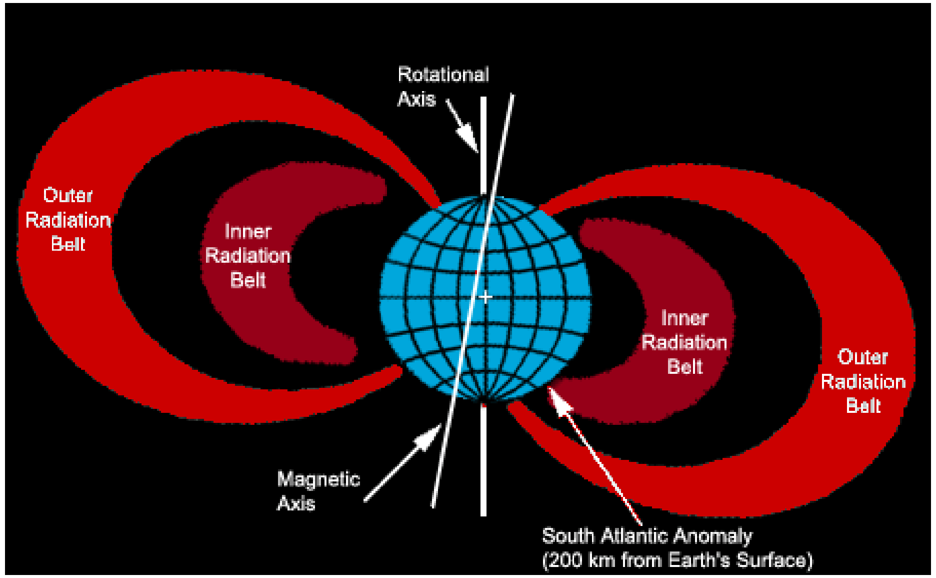

The Van Allen radiation belts consist of two toroidal regions where energetic electrons and protons are trapped in the Earth's magnetic field.

Particles move along the field lines bouncing up and down between two symmetric mirrors points and drift in longitude towards West (protons) or East (electrons)

- The inner belt is mostly constituted by protons, the outer belt by electrons

- Because of the asimmetry of the geomagnetic field, in the SAA region the distance of the inner radiation belt from the Earth surface is only 200 km causing a significantly increased flux of energetic particles that can be harmful to manned and unmanned missions.

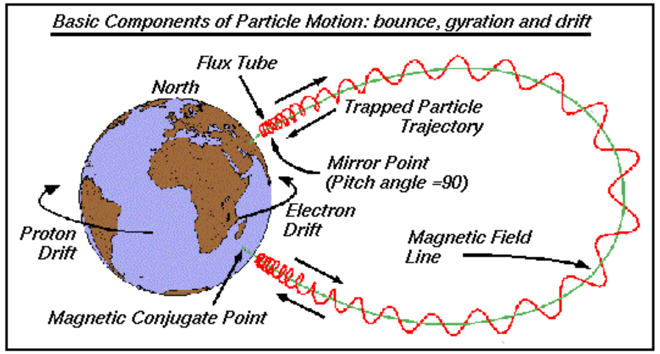

Project Responsible for INFN Firenze C. Grimani

Proton spectra

Protons trapped in the inner belt have kinetic energy up to a few GeV

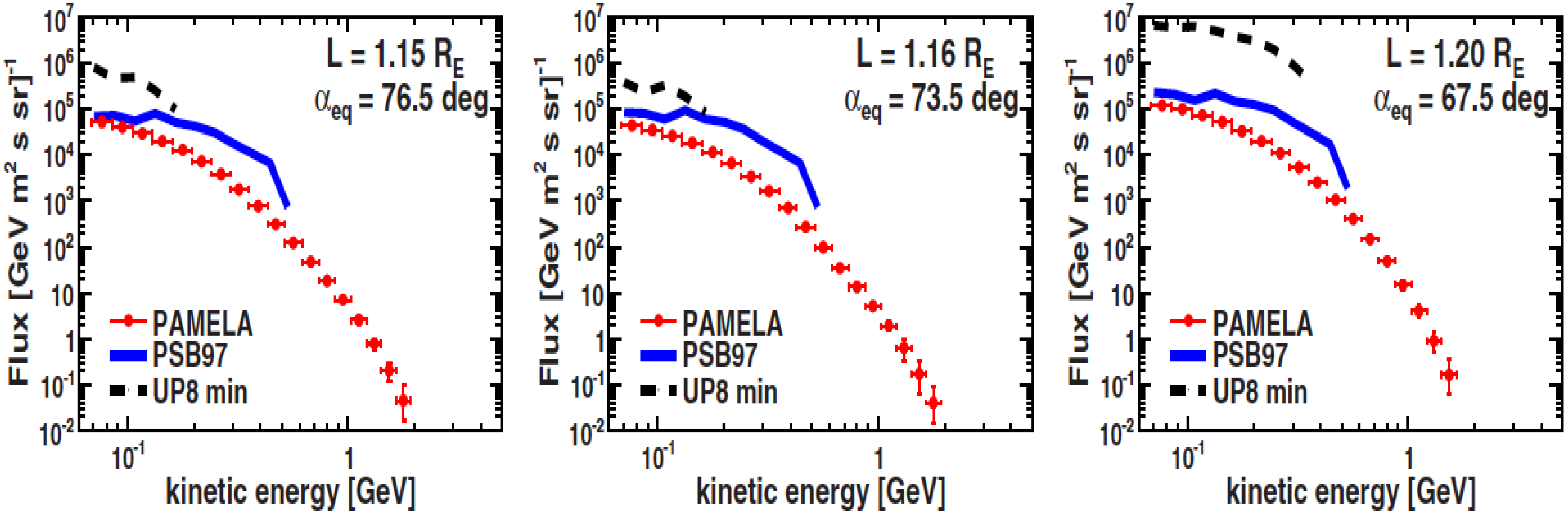

Proton spectra measured by Pamela at different distances fron Earth in the inner belt *O. Adriani et al., ApJ, 799, L4, 2015*

Project Responsible for INFN Firenze C. Grimani

Proton flux measured by Pamela

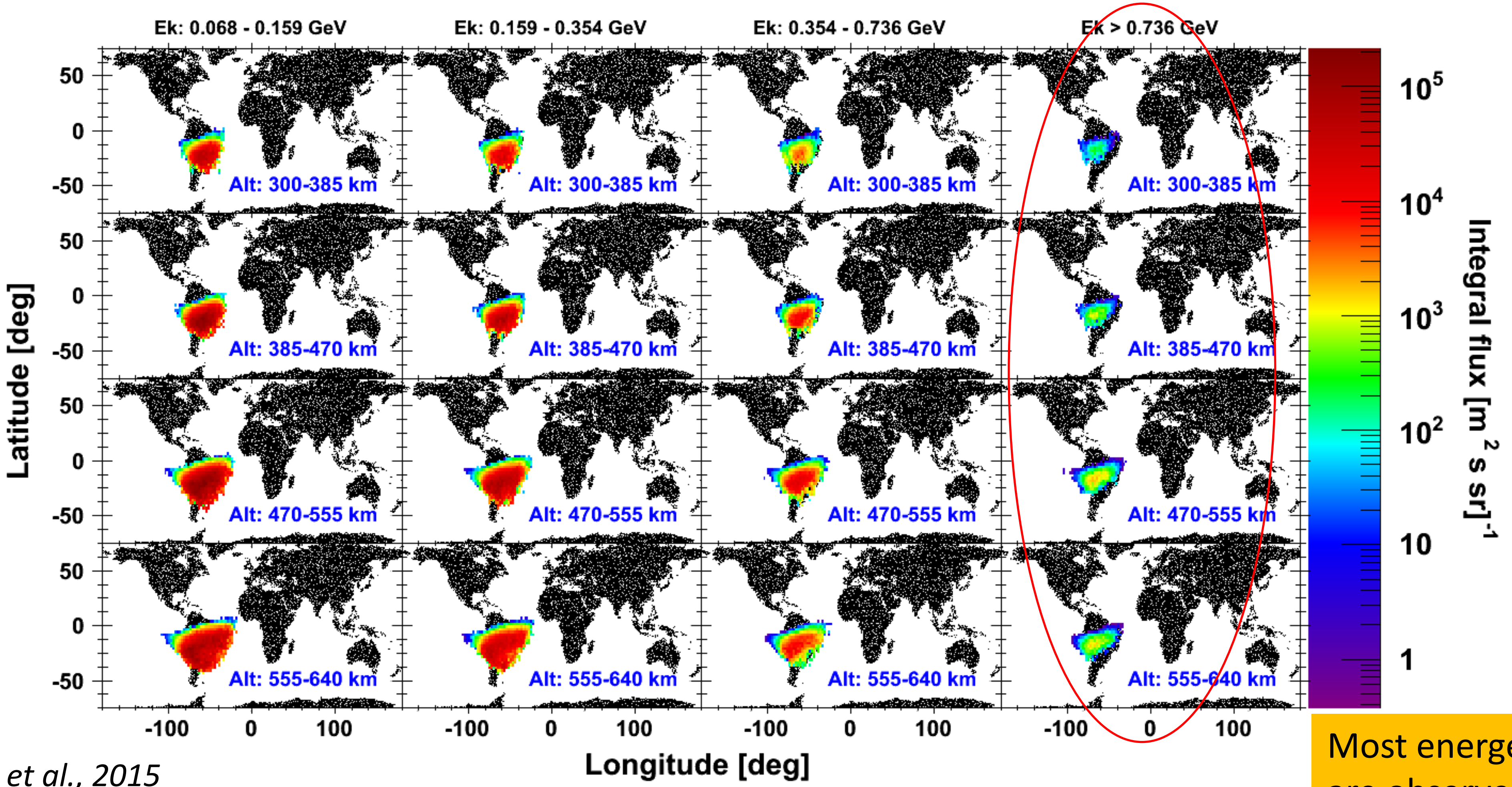

O.Adriani et al., 2015

Most energetic protons are observed above Bolivia and Argentina

Project Responsible for INFN Firenze C. Grimani

Particle precipitations from Van Allen belts

One of the main aim of the SAMADHA project is to verify whether proton precipitations from the inner belt, interacting with the atmosphere nuclei, can produce secondary particles (in particular neutrons) reaching the ground at high altitude in the SAA region, adding a contribution to the environmental dose besides the standard flux of secondary cosmic rays.

Ambient dose equivalent (H*)

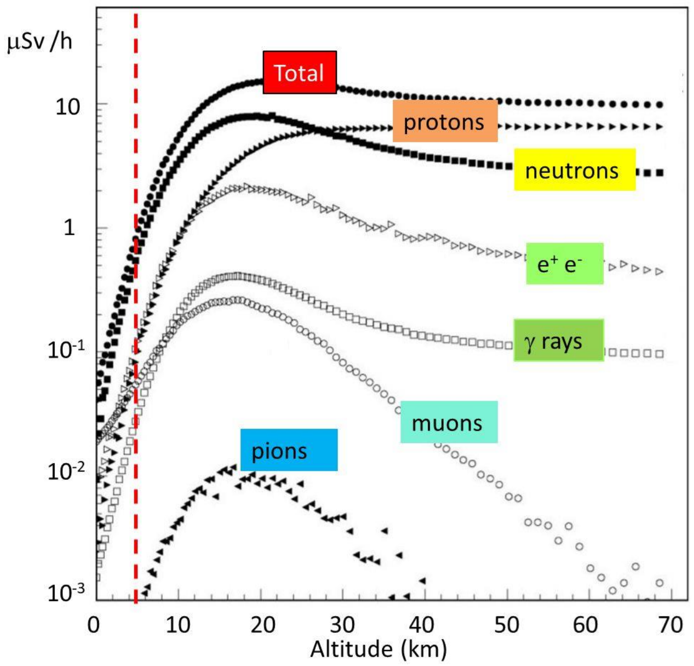

At mountain altitudes, neutrons give the main contribution to the dose rate

Neutron flux increases by a factor 20-30 from sea level to 5000 m

Simulations by Battistoni et al, 2004 with Rv=0.4 GV

Project Responsible for INFN Firenze C. Grimani

Dose rate variations during thunderstorms

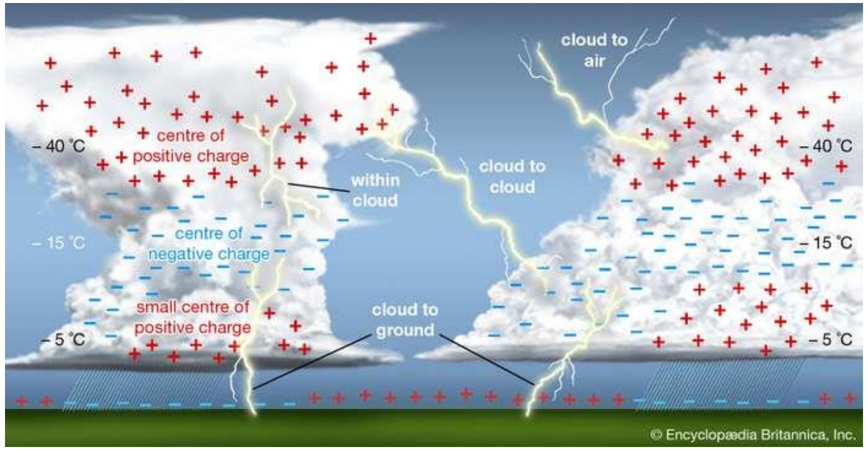

A further aim of the SAMADHA project is to study the dose rate variations during thunderstorms

- Electric fields in atmosphere during thunderstorms accelerate charged particles of secondary cosmic rays
- Significant variations of the flux of all cosmic ray components have been observed by several mountain experiments, but the phenomena are not well understood.
- So far, data on the effects of thunderstorms on secondary cosmic rays at altitudes as high as 5000 m a.s.l. do not exist.

Project Responsible for INFN Firenze C. Grimani

Florence Activity – 2021

Benella et al.; 2020

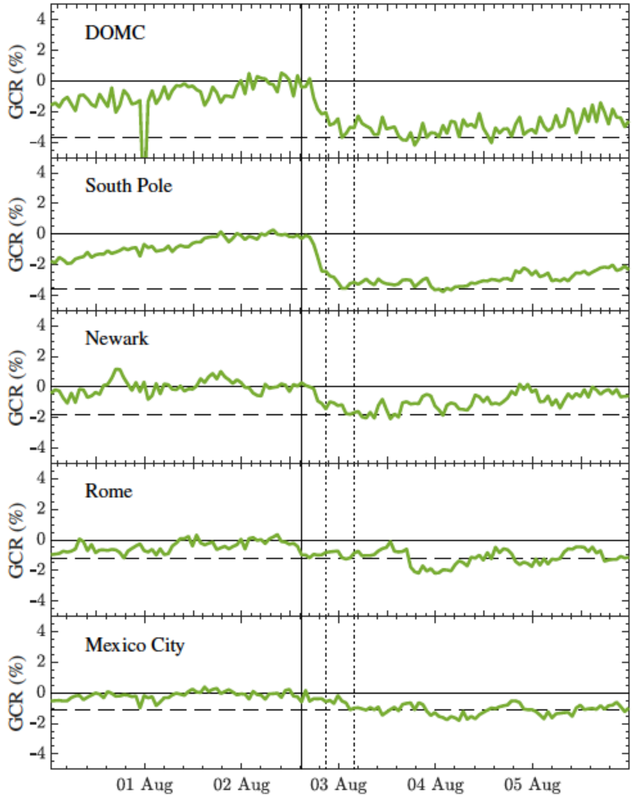

- Analysis of the space-Earth data:
- Study of cosmic-ray variations on Earth and in Space: comparison of Solar Orbiter particle data with Chacaltaya, Terre Adelie, South Pole and DOMC neutron monitors

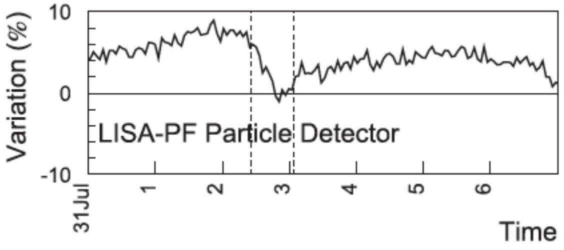

Armano et al.; 2019

- Liulin active dosimeter MC simulation: detector performance at **Laboratorio CNR della Testa Grigia** (Cervinia, Italia, 3460 m a.s.l., 45.95° N, 7.7° E) for comparison of North and South hemisphere measurements

Project Responsible for INFN Firenze C. Grimani

INFN FIRENZE

PERO2: Development of dose monitoring systems based on PEROvskite materials

Sezione di Firenze
M. Bruzzi, A. Vinattieri, C. Talamonti, N.Falsini

"Perovskite" means a class of materials with ABX_3; A,B cations, X anion. Emerging materials for solar cells, LED, photodiode applications, increasing interest as X-ray detector in medical imaging applications*.

Advantages

*Nature 2017 550(7674): 87-91; Physics in Medicine, Vol. 5, 2018 20-23
Adv. Energy Mater. 6 (2016) Nat. Commun. 6 (2015), Adv. Mater. 27 (2015) 41–46.

- **high detection sensitivity (higher than silicon)**
- **high bandgap (2.4eV) defect-assisted thermal generation of e-h pairs negligible**
- **promising transport properties: high diffusion lengths and high charge carrier mobilities;**
- **Thin film deposition on any kind of substrates, also flexible;**
- **process driven by solar cells and LED technology;**
- **potentially defect-tolerant, less prone to mid-gap states as Si, GaAs, InP..**

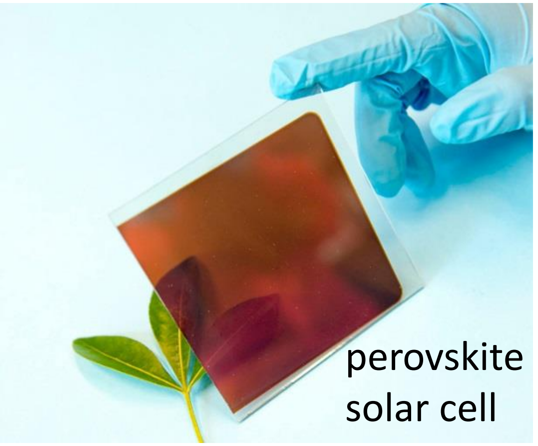

Disadvantages

- **Non tissue equivalent material;**
- **Radiation damage and possible ageing not yet investigated;.**

Project Responsible M. Bruzzi

$CsPbBr_3$

Sensitivity per unit volume : $S = \frac{Q}{D\ \text{Volume}} = \frac{qG}{R}$

$G = \frac{R\rho}{E_i} \quad \rightarrow \quad \boldsymbol{S = \frac{q\rho}{E_i}}$. higher than predicted by the Klein rule

G = generation rate e – h pair;
R = dose - rate ; q = electron charge; ρ = density ;
E_i = mean ionization energy).

	IC(AIR)	SILICON	DIAMOND	CsPbBr3
ρ [g/cm³]	1.29×10^{-3}	2.33	3.52	4.55
E_i [eV]	34.00	3.60	16.20	5.30
S [nC/Gymm³]	0.038	647.22	217.28	**860**

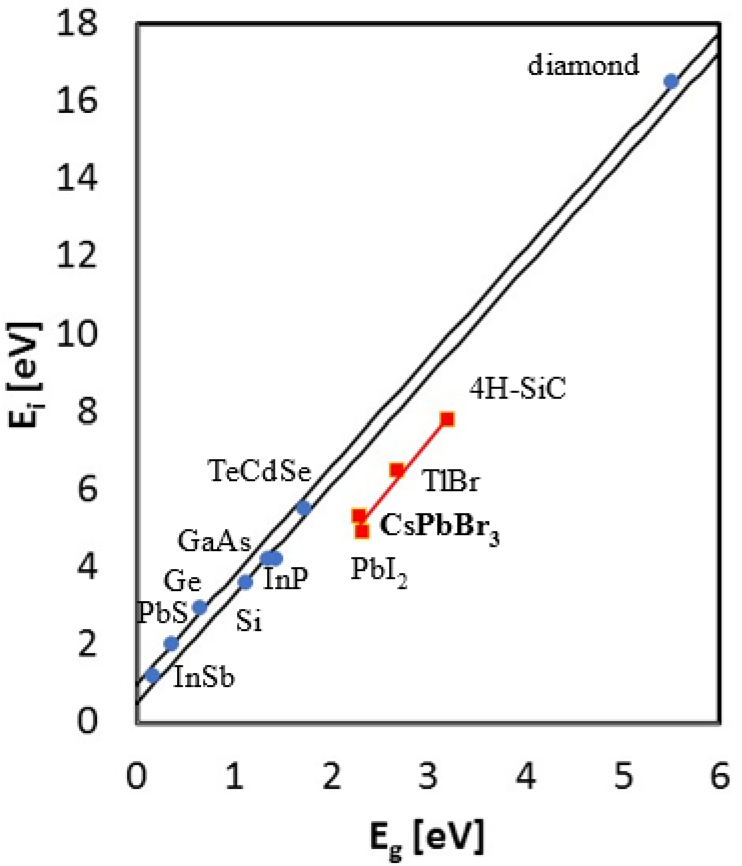

M. Bruzzi and C. Talamonti, Frontiers in Physics, in press

Experimental determination with high resolution gamma detectors shows a significantly lower value E_i = 5.3eV then predicted using Klein's relationship (energy gap E_g = 2.4eV at 300K).

Project Responsible M. Bruzzi

Defects in $CsPbBr_3$ mainly shallow

Conventional semiconductors GaAs, CdSe, InP, are defect intolerant as prone to mid-gap state formation.

Defects in CsPbBr3 are mainly shallow and their capture cross section low ($10^{-19}cm^2$ against typical $10^{-15}cm^2$).

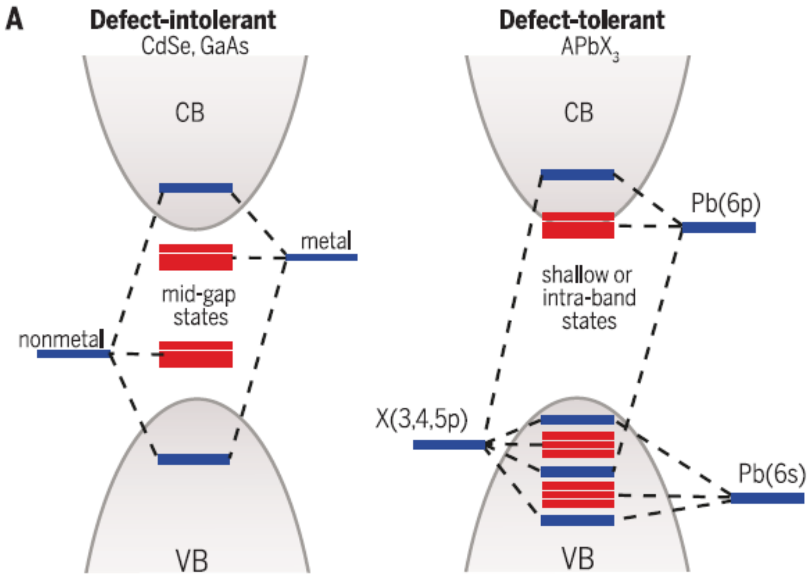

Fig. 4. Defect tolerance in LHP NCs. (**A**) Schematics comparing electronic structures that are defect-intolerant, such as for conventional semiconductors (for example, CdSe, GaAs, and InP), and defect-tolerant, such as for LHPs (*27*). Defects do not act as trap states in LHPs and are therefore benign toward their electronic and optical properties. [Adapted from (*27*)] (**B**) Electronic structure diagrams for $CsPbBr_3$ NCs at the DFT/PBE level of theory (*26*), where PBE is Perdew-Burke-Ernzerhof exchange-correlation functional. Each line

Kovalenko *et al.*, *Science* **358**, 745–750 (2017)

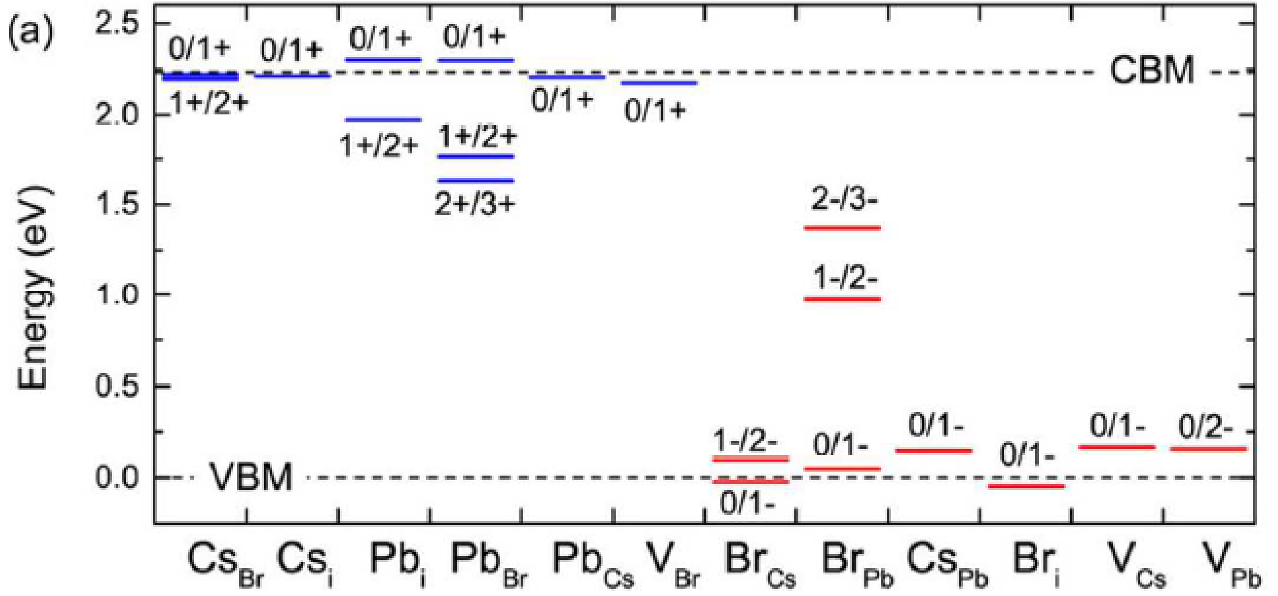

J. Kang, L.-W. Wang, *J. Phys. Chem. Lett.* **2017**, *8*, 489–493.

Project Responsible M. Bruzzi

CsPbBr$_3$ deposition/Growth performed at Florence University

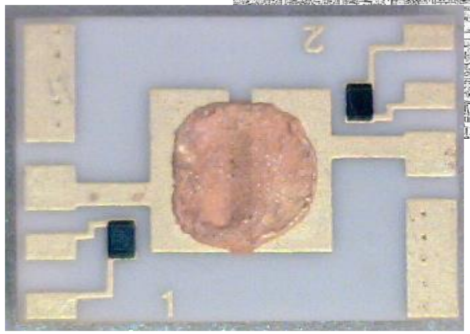

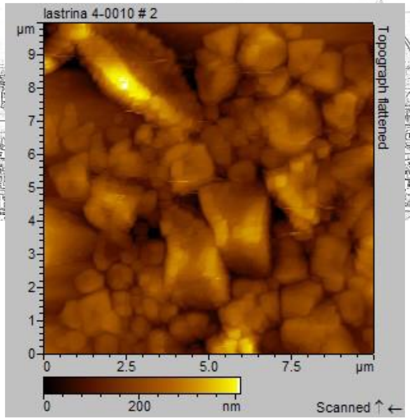

Dropcasted from saturated solution of the CsBr and PbBr$_2$ 1:1 molar ratio in DMSO. Polycrystalline material with grains of the order of a few microns.

Polycrystalline Solvent/anti-solvent procedure from same saturated solution placed in a glass crystallizer covered with paper filter and glass Petri dish. inserted into a second glass container with hermetic closure with an antisolvent. Penetrating in innermost container slowly precipitates the perovskite. Polycrystalline material with grains of the order of a hundred microns.

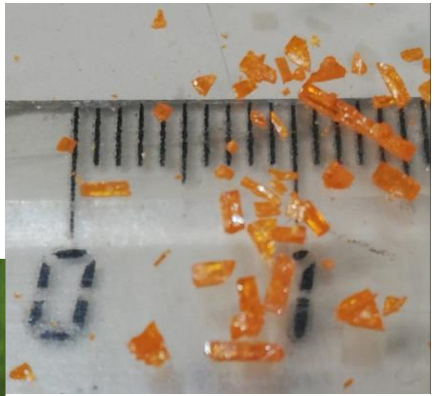

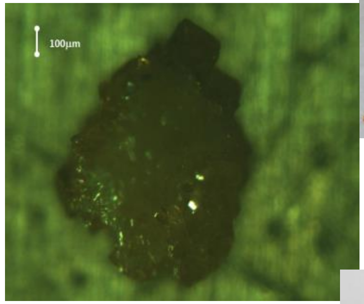

RF-Magnetron sputtering

First time in literature successful deposition of thin (70 nm) CsPbBr$_3$ films starting from single perovskite target. Obtained film uniform and transparent, highly textured and optical properties of film similar to bulk materials.

First Proof-of-Principle of Inorganic Lead Halide Perovskites Deposition by Magnetron-Sputtering

Claudia Borri [1,2], Nicola Calisi [1,2], Emanuele Galvanetto [1,2], Naomi Falsini [2,3], Francesco Biccari [3,4], Anna Vinattieri [2,3,4,5], Giuseppe Cucinotta [6] and Stefano Caporali [1,2,*]

nanomaterials

Project Responsible M. Bruzzi

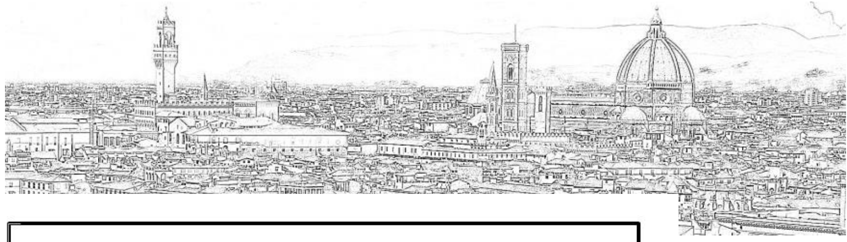

Dropcasted $CsPbBr_3$: charge/current response vs dose/dose rates

Linac beam X (6-25MV)
Dipartimento di Scienze Biomediche Sperimentali e Cliniche "Mario Serio" Università di Firenze

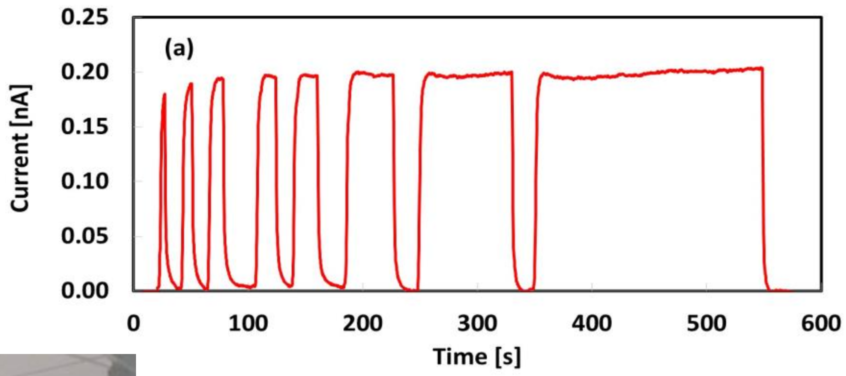

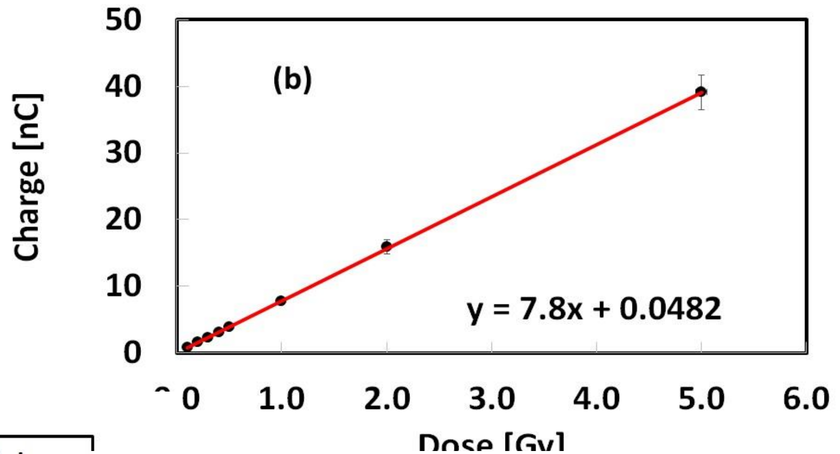

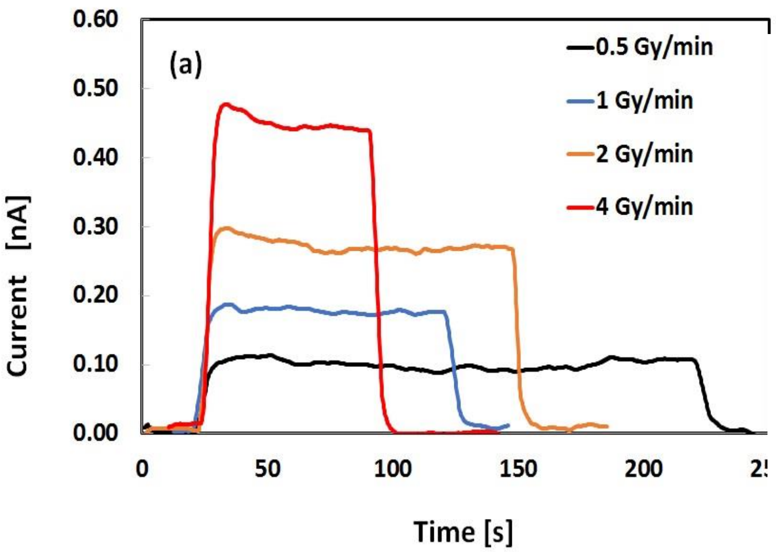

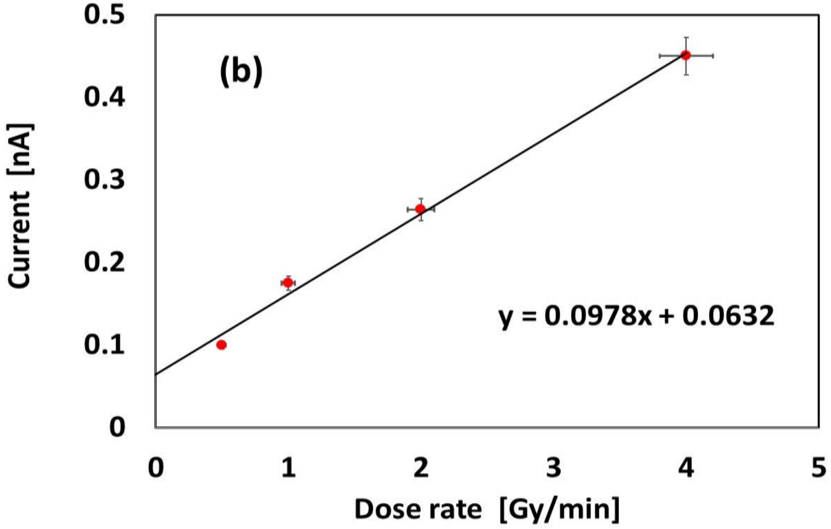

Project Responsible M. Bruzzi

$$s = 69.8 \frac{nC}{Gy \cdot mm^3}$$ Sensitivity lower than predicted probably due to defects at grain boundaries

Dropcasted $CsPbBr_3$ promising response under IMRT beams

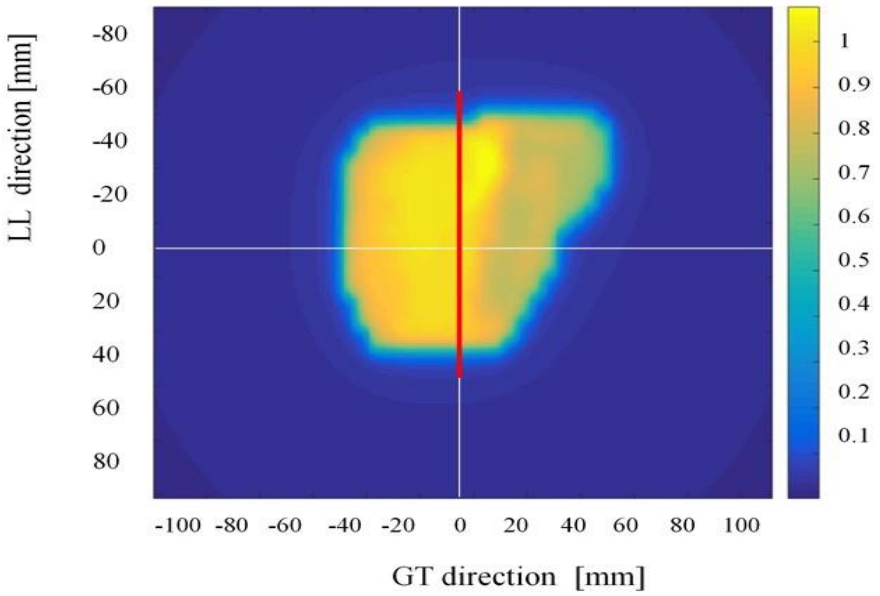

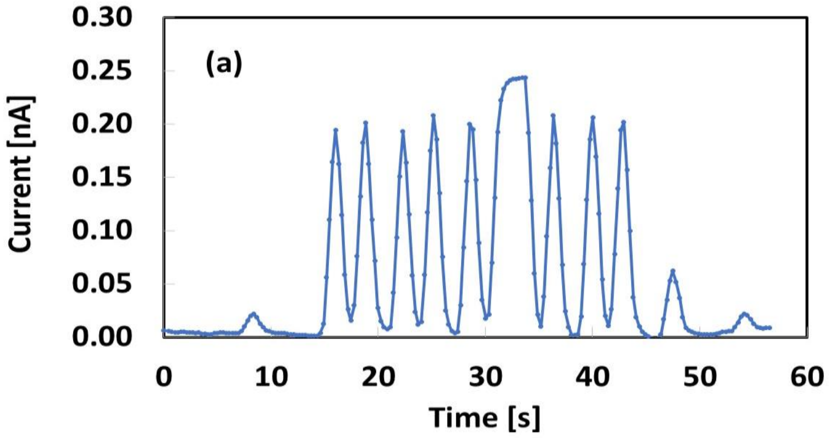

mappa di dose TPS tipica di un cancro alla prostata GT = Gantry Target direction; LL=lateral–lateral direction (isocentro all'intersezione. La linea rossa indica il profilo misurato con dosimetro a perovskite

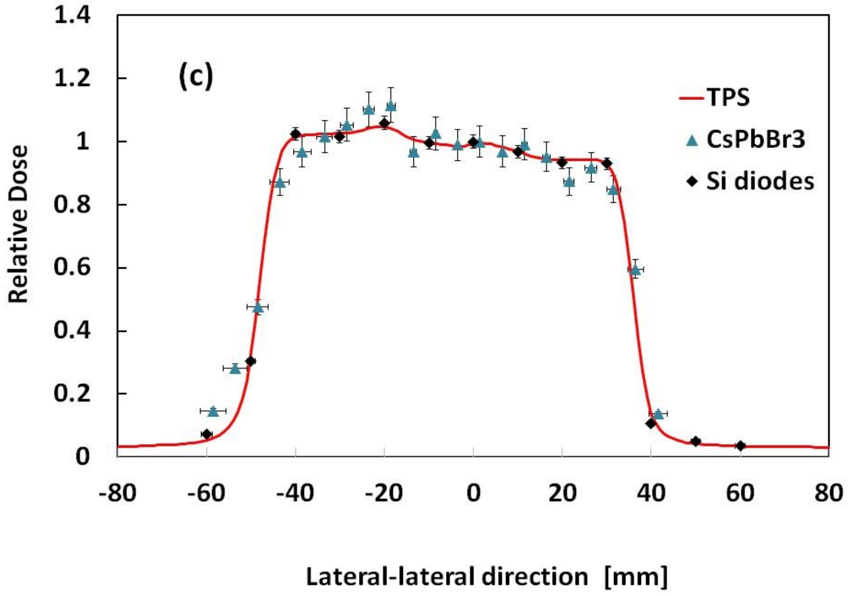

First proof-of-principle of inorganic perovskites clinical radiotherapy dosimeters

Project Responsible M. Bruzzi

Cite as: APL Mater. **7**, 051101 (2019); https://doi.org/10.1063/1.5083810
Submitted: 30 November 2018 . Accepted: 02 April 2019 . Published Online: 03 May 2019

Mara Bruzzi, Cinzia Talamonti, Nicola Calisi, Stefano Caporali, and Anna Vinattieri

Thermally Stimulated Current

Study how defects influence photoconductivity

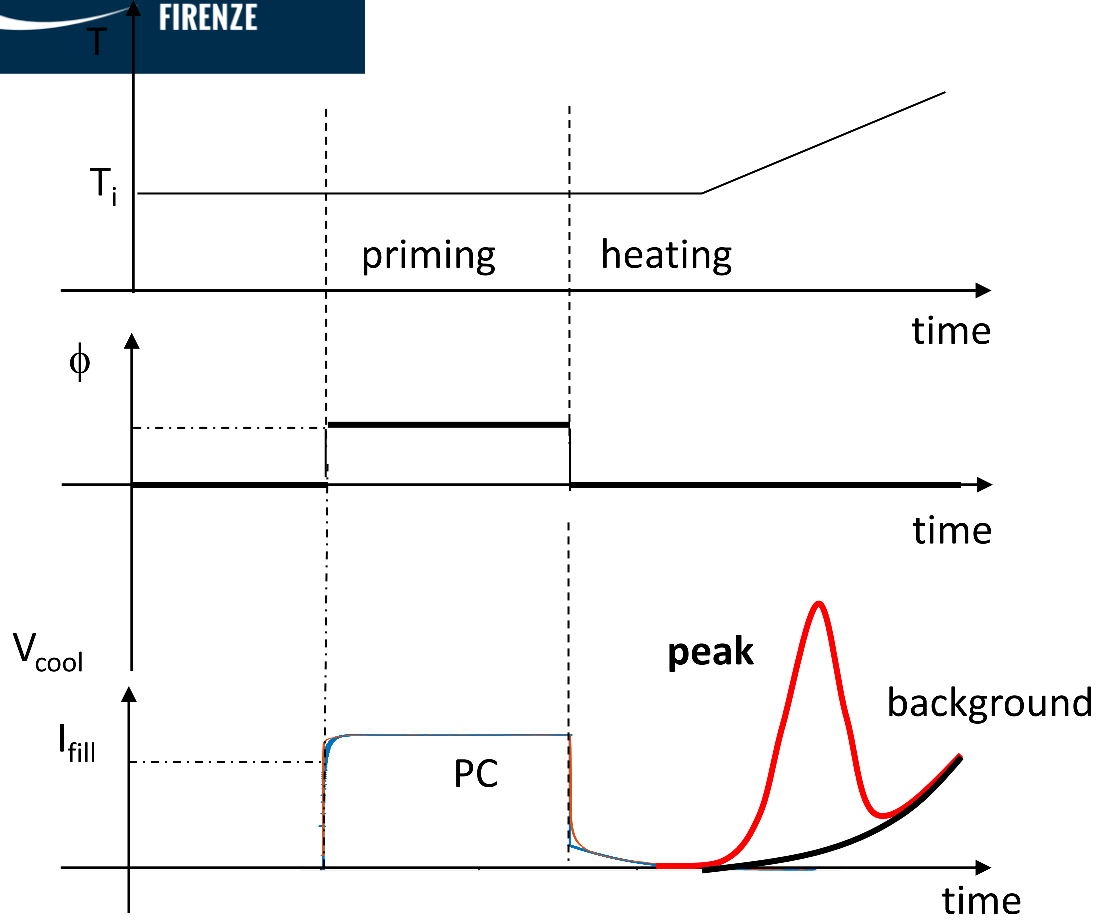

Deep defect 0.45eV influencing room temperature conductivity present only in dropcasted samples

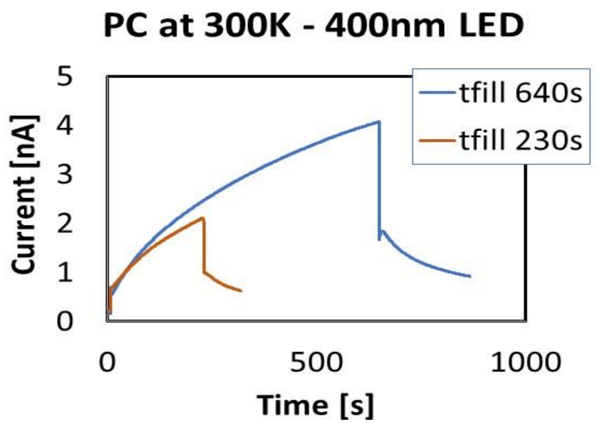

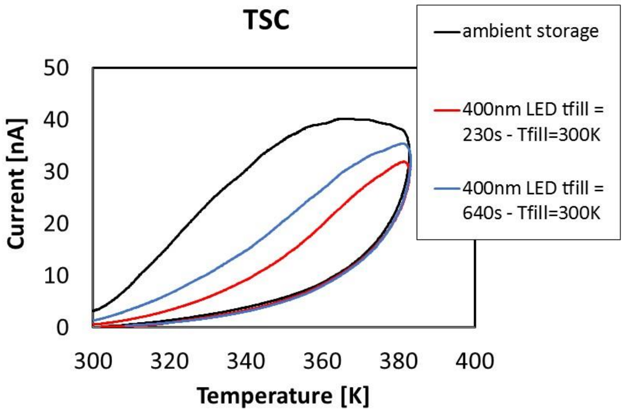

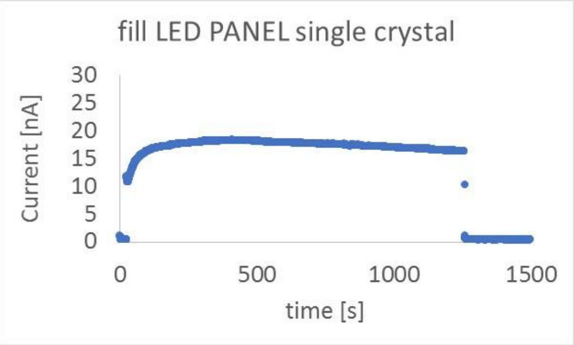

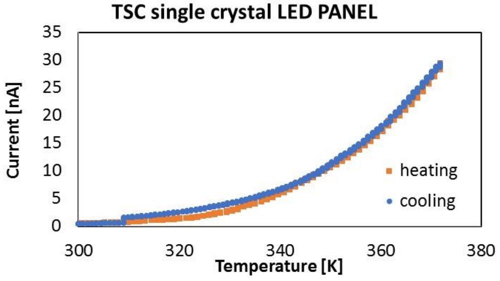

Thermally Stimuated Current peak due to charge emitted from trap during heating; background due to thermal generation rate, same during heating and cooling.

Project Responsible M. Bruzzi

M. Bruzzi et al. Nanomaterials (2019) , Energies (2020)

Crystalline $CsPbBr_3$

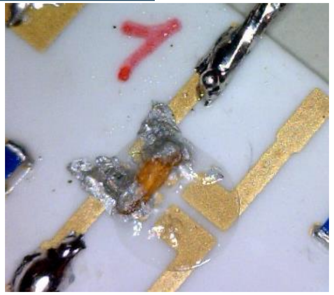

- Better stability due to lower defect density
- Higher miniaturization of the point dosimeter (less than 1mmx1mm active area)
- Low concentration of defects -> better stability during irradiation
- Need to increase grain dimensions up to about 500μm.
- Optimizing packaging in progress

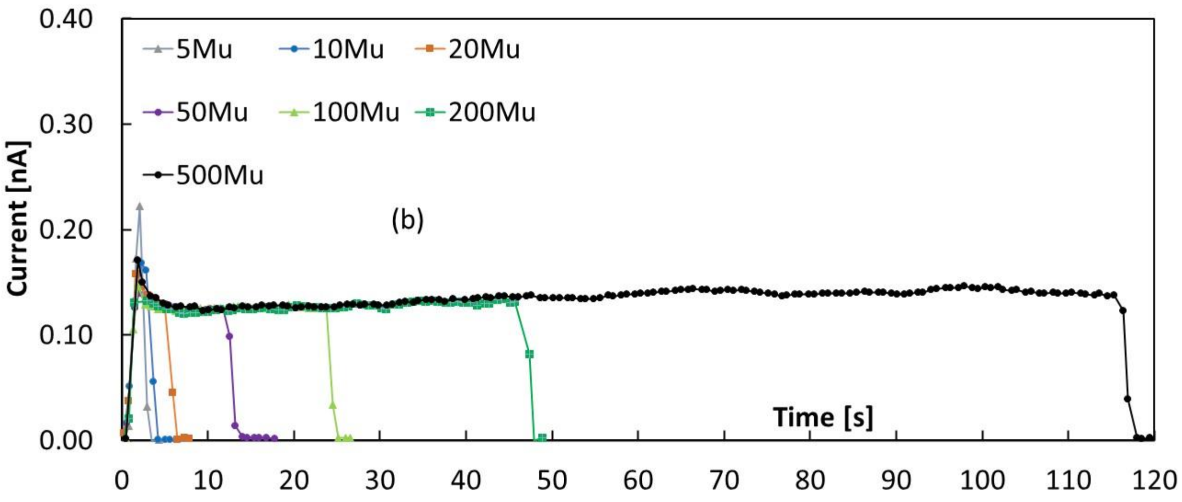

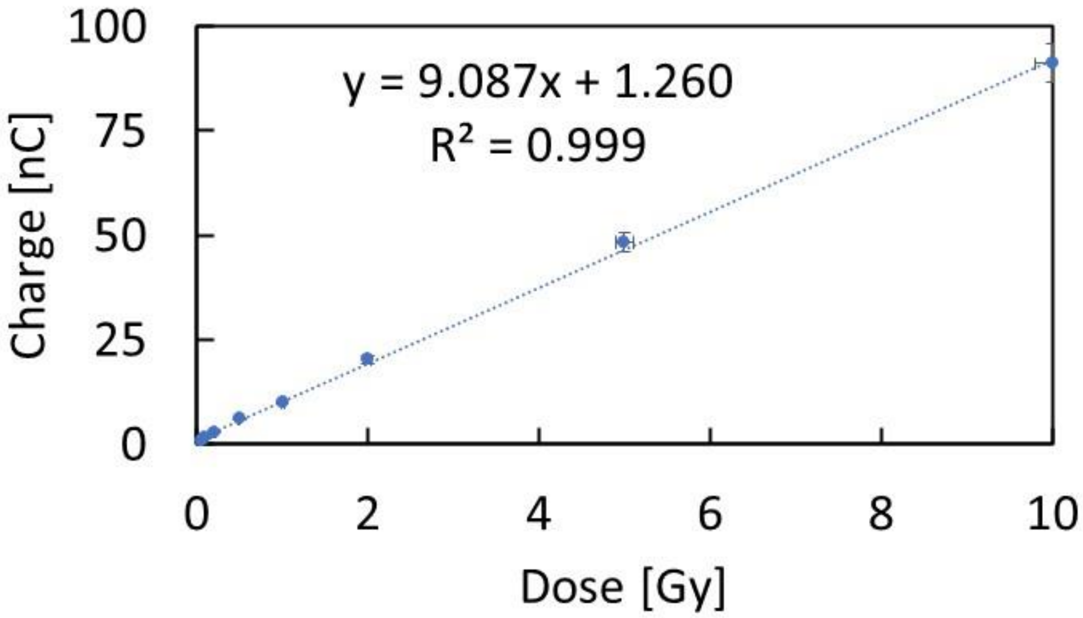

Project Responsible M. Bruzzi

M. Bruzzi and C. Talamonti , Frontiers in Physics, in press.

RF-magnetron sputtered $CsPbBr_3$ devices will be manufactured/measured in 2021

3D-SiAm

Sezioni: Perugia, Firenze, Lecce

- Development of a dosimeter based on a-Si:H thin layers deposited on flexible insulator substrates with pixel / strip topology.
- Transmission measurement of fluxes delivered by present and foreseable clinical beams.

TRansmission Detectors (TRDs): inserted between radiation source and patient, for an independent monitoring of the dose delivery.

Response of the 2D detector array can be correlated with the amount of 2D energy fluence incident on the patient and therefore with dose distribution.

An ideal TRD device will monitor the incident fluence of particles with high accuracy (2% or less) without perturbing the incoming radiation beam.

Project Responsible for INFN Firenze C. Talamonti

WHY a-Si:H detector?

- highly radiation resistance [1] due to the disordered structure, e.g. if compared to crystalline silicon,
- mature technology (mass production of solar cells [2], memories ,TFT [3] detectors for X-ray imaging),
- wide area and thin detectors can be fabricated in a single step process, avoiding assembling, thinning, positioning, glueing, and bonding issues,
- flexible detectors can be obtained with deposition on a insulating support

Disadvantages

- High depletion voltage (1100 V with 50μm diodes)
- substrato non removibile
- max T processing 250-300 °C
- Low S/N due to 50% CCE with 30 μm and high leakage current (up to 1 uA/ cm^2) .
- Low mobility 1 - 10 cm^2 /Vs elettroni 2 order of magnitude less for holes

1)Radiation hardness of amorphous silicon particle sensors, J. Non-Cryst. Solids 352 1797-800 (2006).
2) Amorphous silicon solar cells,Appl. Phys. Lett. 28 671-3 (1976)
3)TFTs fabricated byXeCl excimer laser annealing of hydrogenated amorphous-silicon film,IEEE Transactions on Electron Devices (Volume: 36 , Issue: 12 , Dec1989)

Project Responsible for INFN Firenze C. Talamonti

a-Si:H in portal imaging systems

Combining the use of the transmission detector and the portal imaging acuqisition system for in vivo dosimetry during the treatment for beam monitoring and dose delivery control

Combined use of a transmission detector and an epid-based in vivo dose monitoring system in external beam whole breast irradiation: A study with an anthropomorphic female phantom Arilli, C., Wandael, Y., Galeotti, C., Pallotta, S., Talamonti, C. Applied Sciences , 2020, 10(21), pp. 1–12, 7611

Project Responsible for INFN Firenze C. Talamonti

Present TRDs are large area ionization chambers

Main issues:

- impact of TRDs on dose received by patient (absorption of radiation, increased surface dose)
- detection sensitivity to a variety of errors (output variation, static MLC positional errors, dynamic MLC positional errors).

Beam perturbation and dosimetric effects on patients are quantified by measuring transmission of radiation and changes in the percentage depth dose (PDD) profiles, including the buildup region and the surface dose.

- Large area ionization chamber with a gradient in the electrode plate separation (in the axis of MLC motion)
- Inclinometer for gantry and collimator angle measurement
- Wireless connection

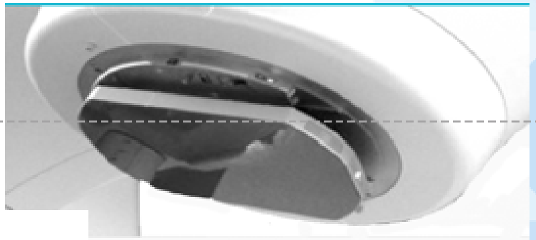

Table 1: Comparison between ionization chamber TRD

	Transmission factor at 6 MV	Increase in surface dose at 6 MV (SSD 90cm)	Source-detector distance (cm)
DAVID	0.928 to 0.939	1.03	44
COMPASS	0.967	1.20	65
DOLPHIN		1.20	65
IQM	0.93	1.15	64
Sc. Fibers (SF)	0.983	1.10	64

Project Responsible for INFN Firenze C. Talamonti

3D-SiAm
Preliminary phase

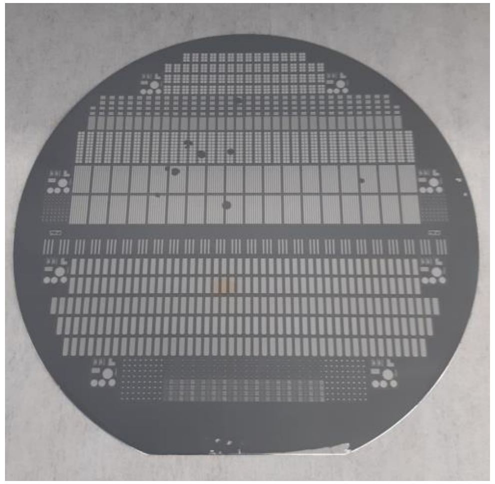

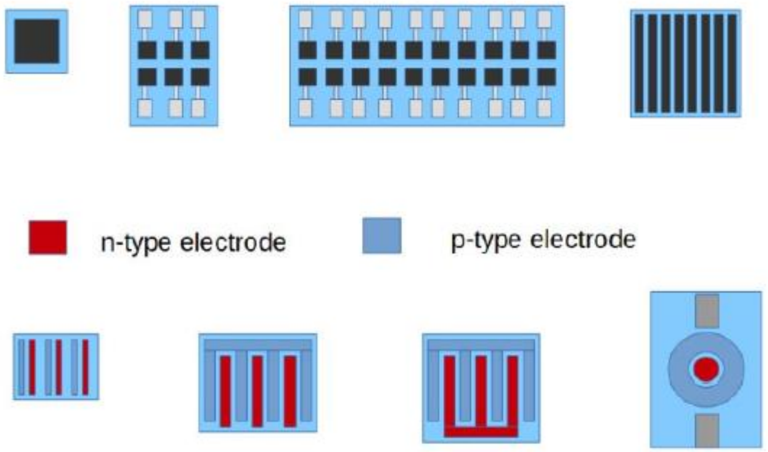

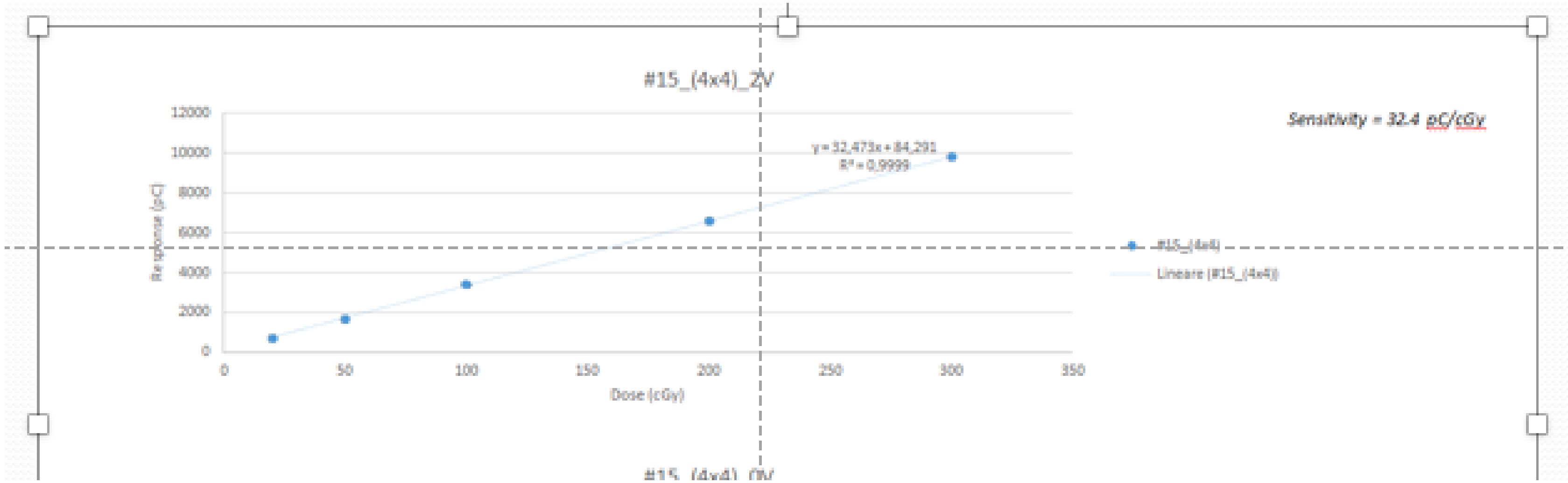

Project Responsible for INFN Firenze C. Talamonti

3D-SiAm
Prototype development

Development of planar detectors on kapton substrates for dosimetry and fluxmetry

A low cost (15-20kEur) prototype a-Si:H on kapton will be manufactured by 3D-SiAm with a limited cost (15-20 kE in tutto) in 2021

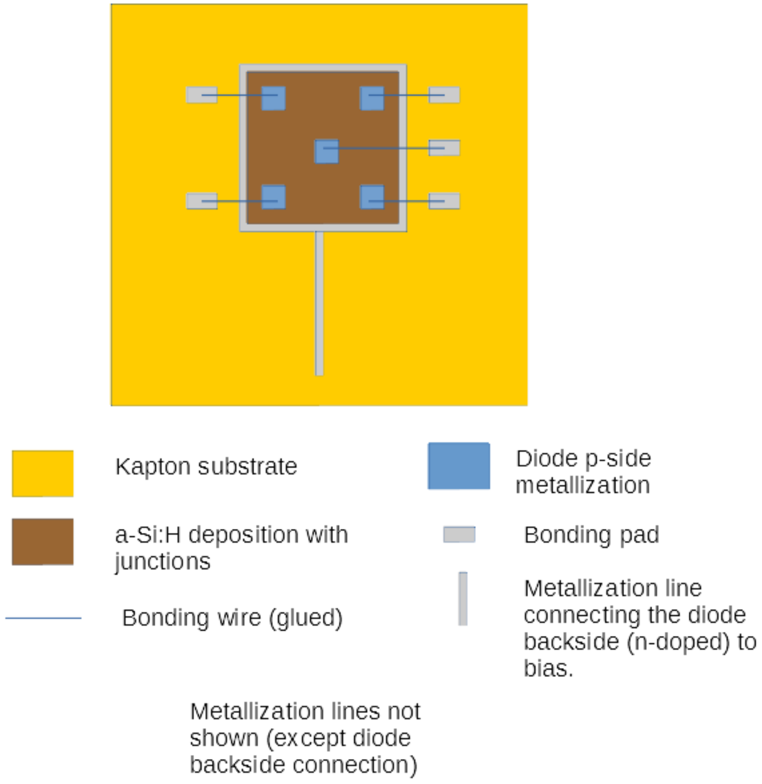

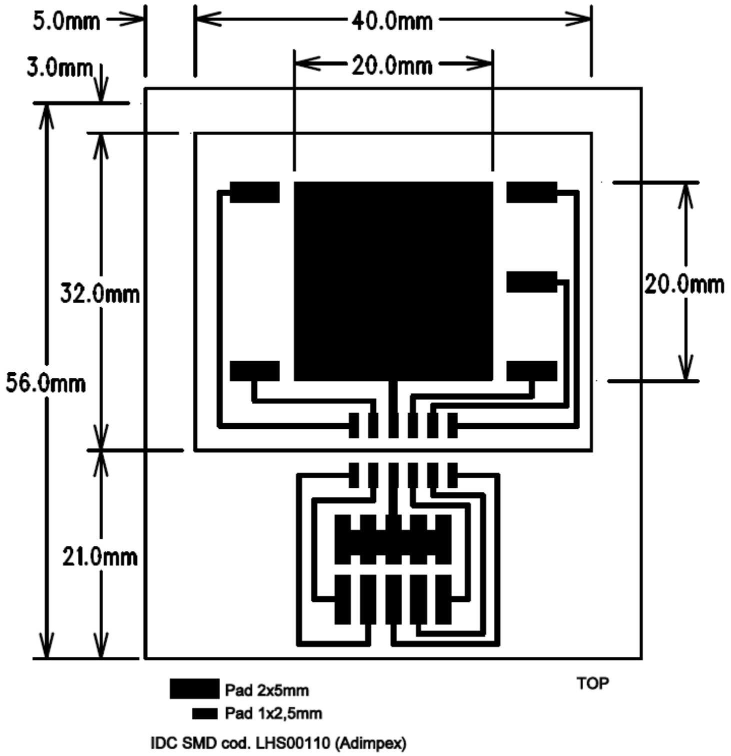

Project Responsible for INFN Firenze C. Talamonti

TimeSPOT and 4D tracking

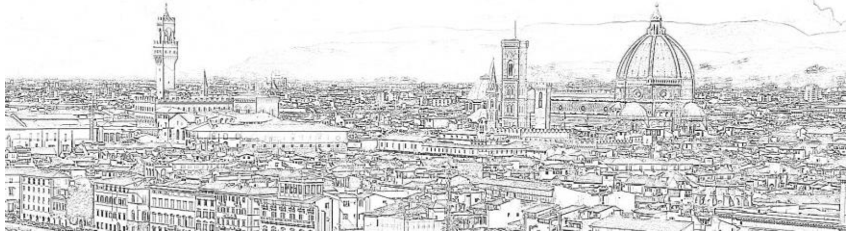

L. Anderlini, M. Bellini, C. Corsi, S. Lagomarsino, C. Lucarelli, G. Passaleva, S. Sciortino, M. Veltri

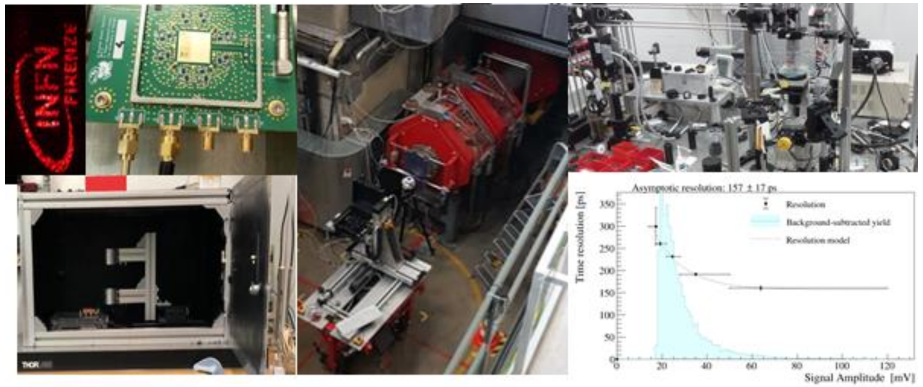

Aim: Development of a demo timing tracker featuring:

- Rad-hard, trench-shaped, **3D silicon detectors** optimised for timing
- Rad-hard, **3D diamond detectors** optimised for timing
- Rad-hard 28-nm **readout electronics** with precise timing resolution
- Fast FPGA-based **backend electronics** to deal with unprecedented data throughput
- Highly parallel **reconstruction algorithm operating on FPGAs** to reduce data throughput towards CPUs

The development of the various parts is being coordinated through common **testing session** to efficiently access test facilities (PSI and CERN for test-beams, Lubjana for neutron irradiation, development timing-optimized Cherenkov counters for reference...).

Project Responsible for INFN Firenze S. Sciortino

Sensor fabrication

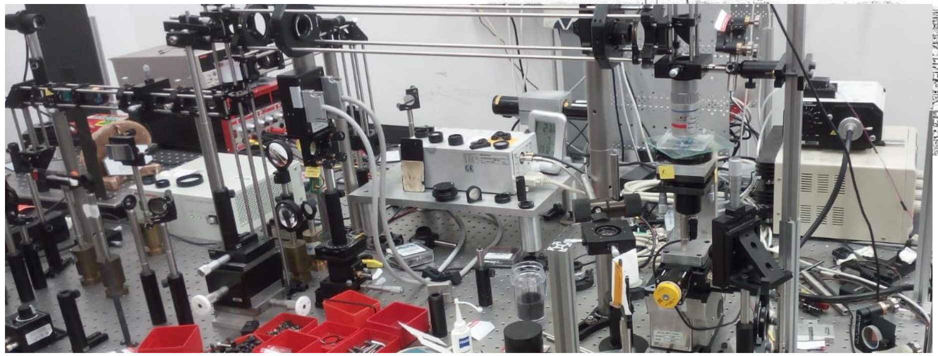

A **800 nm laser with 50 fs pulses** is focussed inside the diamond bulk.

Diamond is transparent at 800 nm, but a sufficiently high light density allows for multiple-photon interactions, opening energy adsorption through large-bandgap transitions.

Adsorbed energy transforms **diamond** into a mixed carbon phase including **graphite**.

Sufficiently **short pulses prevent annealing of graphite** into amorphous carbon (with higher resistivity)

A holographic technique is used to compensate the refraction effects due to the high refractive index of diamond (n = 2.4).

Project Responsible for INFN Firenze S. Sciortino

3D sensors

3D sensors are obtained with graphitization of patterns of electrodes.

Due to the small capacitance of the elementary cells it is customary to short-circuit many electrodes to get large sensitive areas, with good radiation hardness and few readout channels.

Connecting an electrode per electronic channel one gets pixel detectors.

RD42 successfully bump-bonded 3D diamond sensors to readout chips.
Our first attempt planned (with IZM) for 2021.

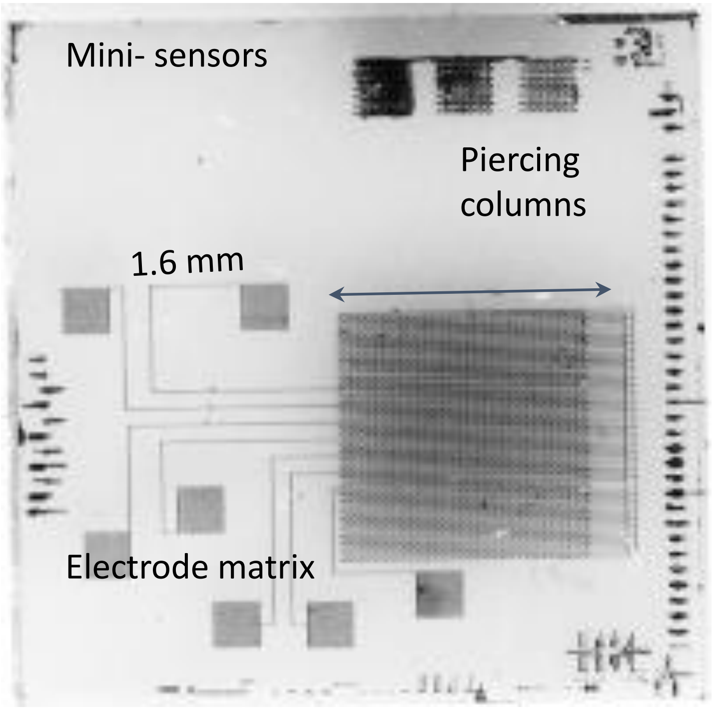

wire-bonding,
graphite pads

Project Responsible for INFN Firenze S. Sciortino

For consistency with TimePix, we use 55 µm pitch

Timing optimization

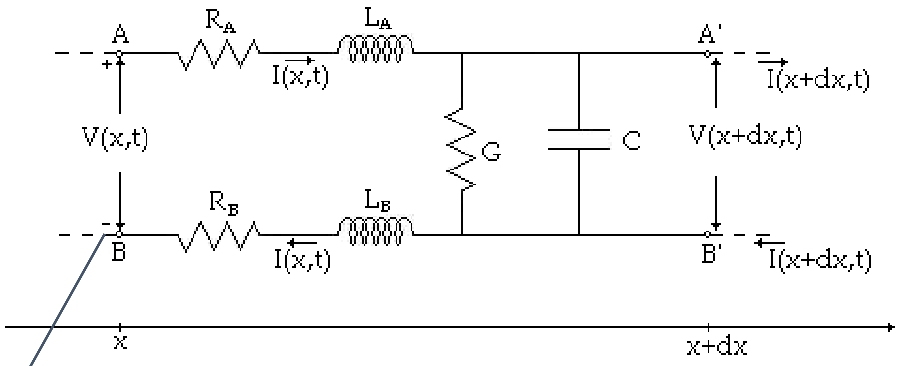

While the drift of charge carriers in diamond is significantly faster than in Silicon, the high resistivity of the electrodes increases the time-constant of the system, giving slower and smaller signals.

To get faster sensors one needs more conductive electrodes.

$$R = \rho \frac{L}{A}$$

Graphitization involves a multitude of graphitic domains, with resistance increased by the connections. Better laser focus enhance the "density" of domains and improves conductivity.

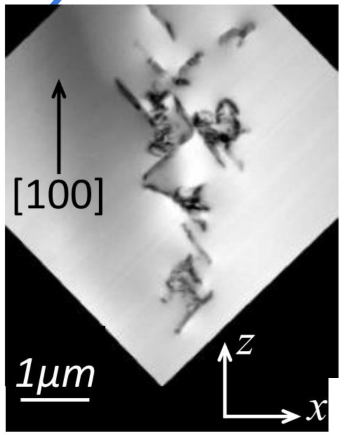

Graphite density is smaller than diamond density: graphitizing inflates and may crack diamond. This limits the column diameter.

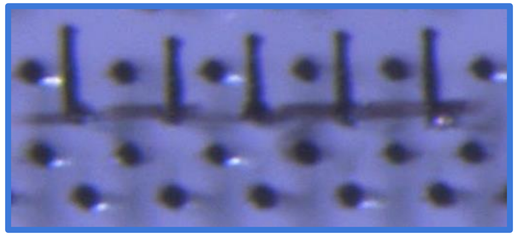

Appl. Phys. Lett. 111, 081103 (2017)

INFN FIRENZE

Test electronics and data acquisition

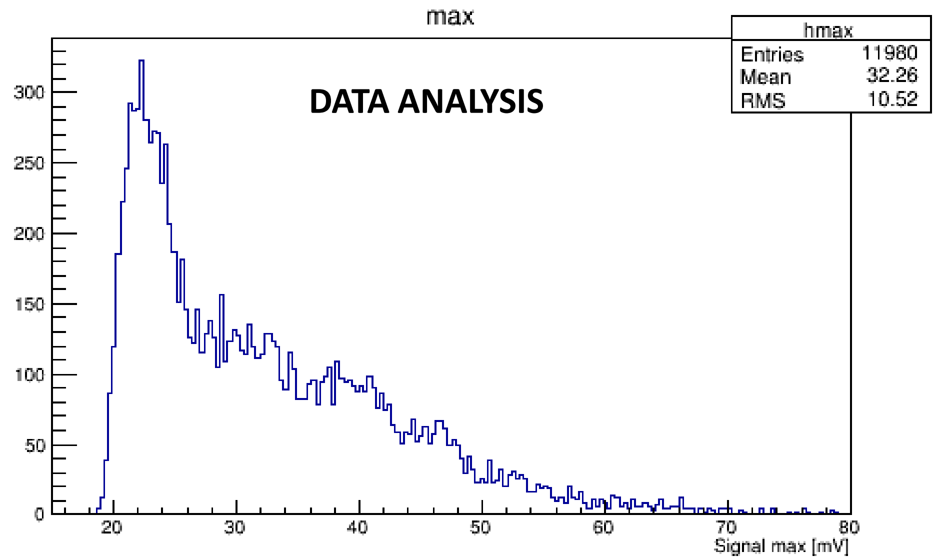

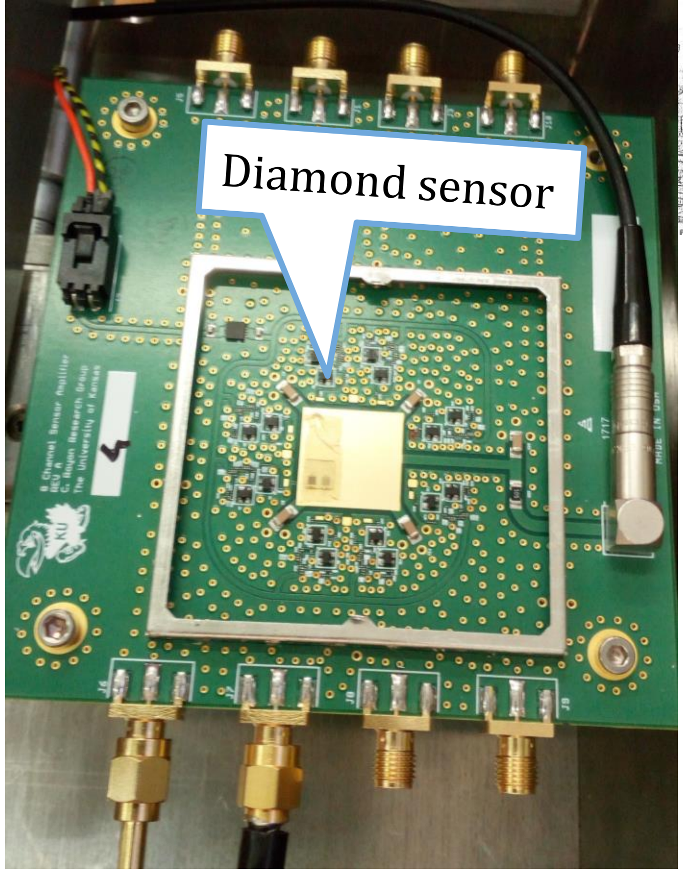

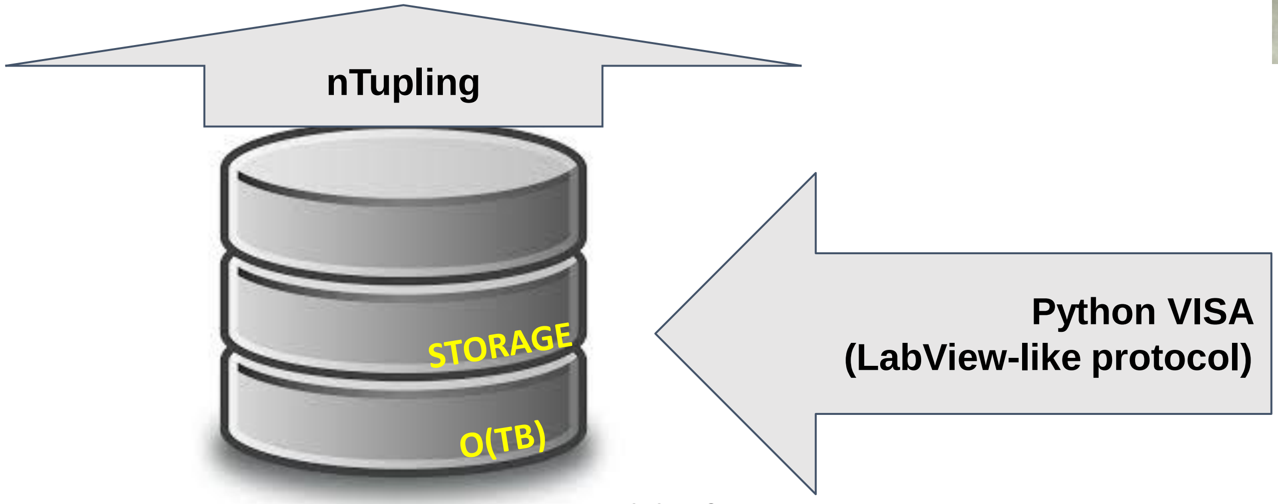

Project Responsible for INFN Firenze S. Sciortino

Timing characterization: *test beam @PSI*

Sensor produced in early 2019

270 MeV/c pion beam

Two Cherenkov counters used to reject non-MIP contributions (mainly protons) below Cherenkov threshold

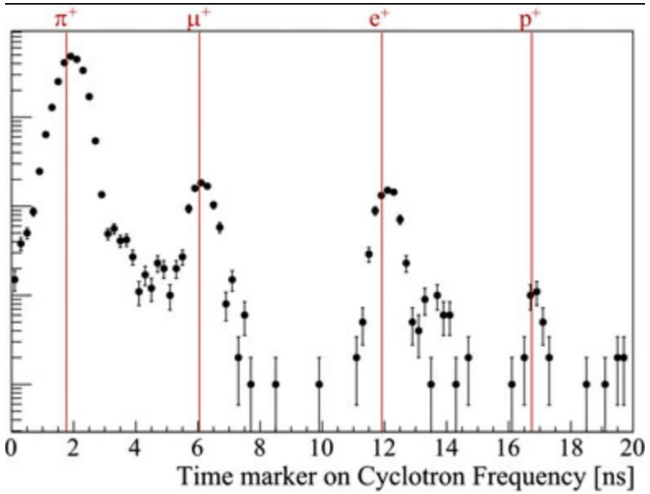

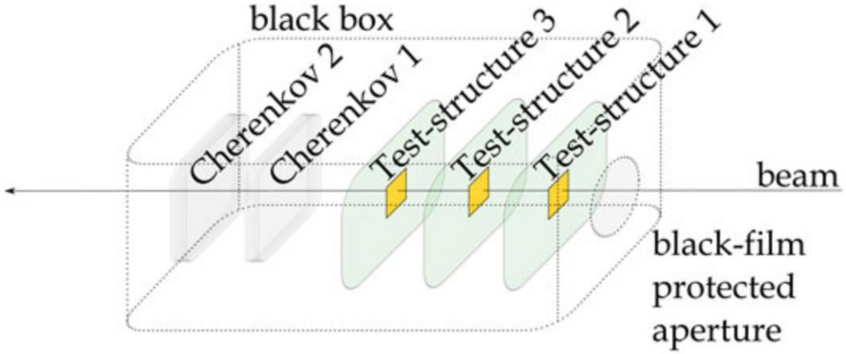

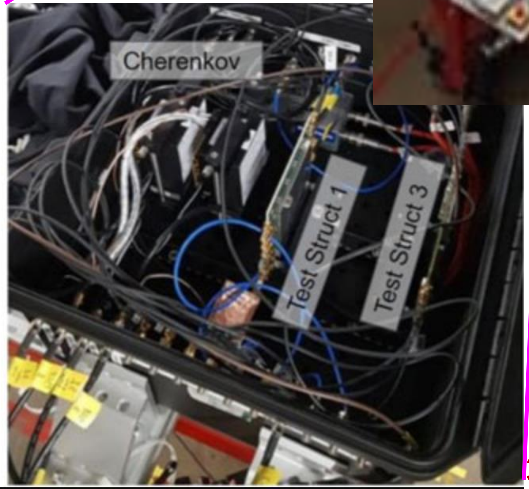

Project Responsible S. Sciortino

Timing characterization: *^{90}Sr setup*

Sensor produced in early 2019

Results obtained at the test beam have been used as standard candle to validate a table-top setup.

Cherenkov counter (an MCP where the radiator is provided by the entrance window) is used to reject non-MIP electrons, selecting only the high-energy tail of the ^{90}Sr ß spectrum.

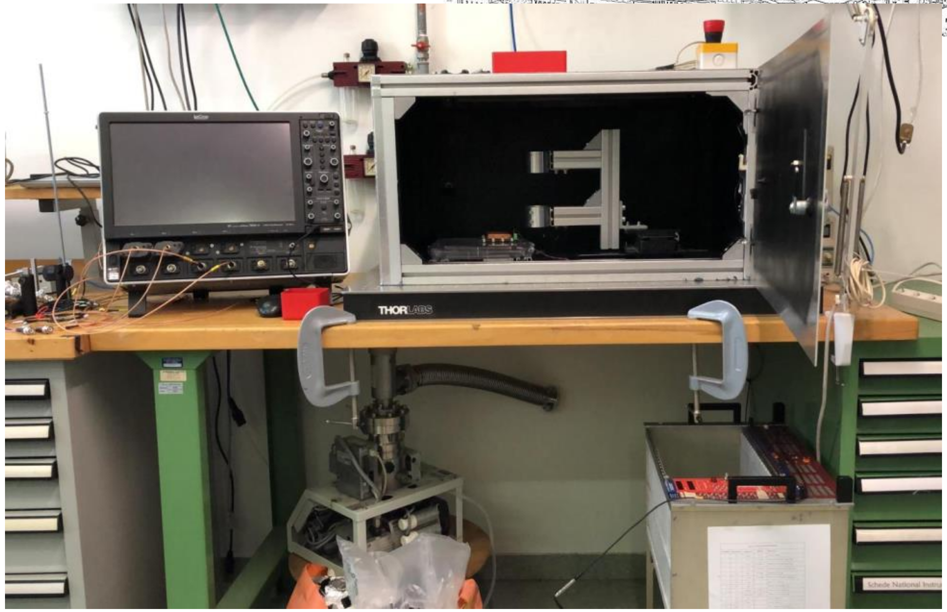

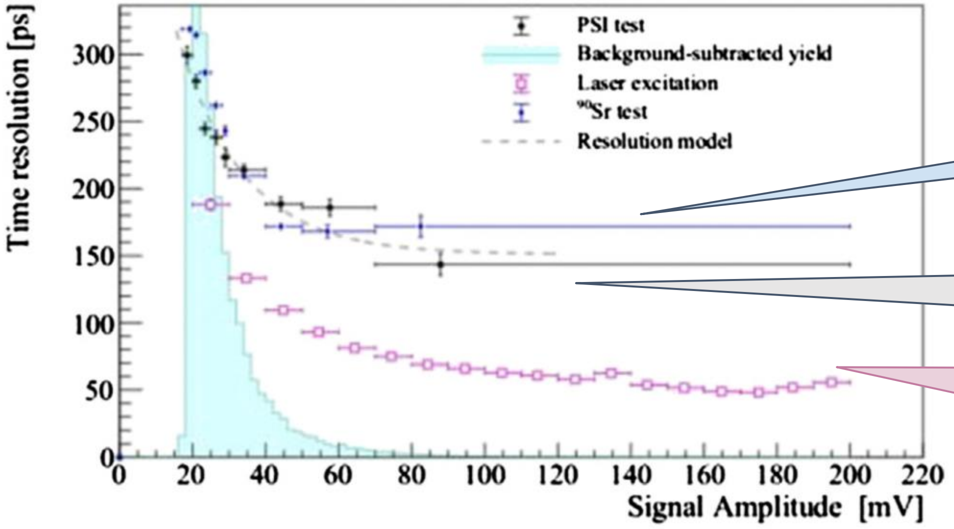

Table-top results with ^{90}Sr source

PSI test-beam results with pions

Results with laser excitations: bad proxy

INFN FIRENZE

A complete upgrade of the optical system since 2019

- A complete new design using a new objective and a new holographic system (adaptive mirror)
- Systematic studies yielded column resistivity ilowerby an order of magnitude with respect to the previous setup
- A first test-sensor made in October made new difficulties in fabrication evident.

Still, the time resolution obtained with the new system “out-of-the-box” is already the same as the diamond sensor produced after years of optimizations with the previous setup.

Due to Covid-19, in 2020 we accumulated some delay, but we are still on track with the rest of TIMESPOT initiative.

In March 2021 we will produce sensors at our best to go through the bump-bonding procedure on the TIMESPOT 28-nm chip and integrate diamond sensors in the demo tracker.

Project Responsible for INFN Firenze S. Sciortino

INFN FIRENZE

Perspectives - for the discussion

- If fabrication principle is demonstrated and time resolution goal is achieved, next step is to upgrade to a large scale (area + number of sensors) production procedure. Need an improved setup: better and more versatile laser, improved optical system etc.
- Other R&D directions - material studies
  - Polycrystalline sensors - cheaper, larger area - do they work in 3D ? time resolution ?
  - DOI (diamond-on-iridium): new promising growth technology - midway between sCVD and pCVD
- Applications (besides the “institutional” HEP applications)
  - Neutron detectors in hostile environment (e.g. fusion reactors) - but also TOF in facilities like e.g. ESS or nToF
  - (μ-) dosimetry
  - …(other applications like e.g. color centers for quantum technologies etc studied by Stefano, Silvio and CNR-INO)

Project Responsible for INFN Firenze S. Sciortino

CONCLUSIONS

- The field of detector & dosimeters development and their applications is a primary focus in CSN5;
- Consolidated expertise of INFN Firenze, accumulated also by other groups
- Can be further expanded in future by increasing sinergy within our scientific community